Available online at www.sciencedirect.com
SCIENCE DIRECT®
International Journal of Heat and Mass Transfer 47 (2004) 3119–3129
International Journal of HEAT and MASS TRANSFER
www.elsevier.com/locate/ijhmt

Temperature distribution and heat transfer characteristics of an inverse diffusion flame with circumferentially arranged fuel ports

L.K. Sze, C.S. Cheung, C.W. Leung *

Department of Mechanical Engineering, The Hong Kong Polytechnic University, Hong Kong, Hung Hom, Kowloon, China

Received 5 September 2003; received in revised form 13 February 2004
Available online 17 April 2004

Abstract

Experiments were conducted on IDFs burning butane. The flame holder has a central air jet surrounded by 12 circumferentially arranged fuel jets. The flame consisted of a short entrainment zone and a long mixing and combustion zone with intense combustion. The temperature profiles of the flame showed a cool core at low flame heights, which disappeared at high flame heights. The stagnation point heat flux and radial heat flux distribution of the same flame, upon impinging on a flat plate, also indicated a cool core at low nozzle-to-plate distance but disappeared at high nozzle-to-plate distance.

Keywords: Inverse diffusion flame (IDF); Butane/air combustion; Heat flux; Impingement heat transfer; Nozzle-to-plate distance

1. Introduction

Diffusion flame is one of the most basic flame configurations in combustion. Numerous investigations have already been carried out in understanding the characteristics of the flame [1]. The IDF is a kind of diffusion flame with an inner air jet being surrounded by outer fuel jet(s). If the air jet velocity is high enough, the fuel at the outer jet(s) will be entrained inward and mixes with the air to form a combustible mixture.

The first comprehensive study on IDF was conducted by Wu [2], who classified the IDF into six types according to the appearance and stability of the flame. Bindar and Irawan [3] investigated the size and structure of LPG and hydrogen IDF at high level of fuel excess under unconfined condition. The shape of the IDF was different from that of Wu [2], consisting of a broader base and a narrower tower. He reported that the shape and height of the IDF was found to be affected by the ratio of fuel rate momentum to air rate momentum. Clausing et al. [4] investigated the stability characteristics of the IDF. They used a modified Peclect number as a practical tool for understanding and predicting the extinction characteristics of IDF. Takagi et al. [5] reported that the maximum temperature of IDF was higher than the usual diffusion flame at different flame heights. Sidebotham and Glassman [6] investigated the soot formation characteristic of IDF under the effect of temperature, fuel structure and fuel concentration, and found that soot formation was lower in the IDF.

One of the applications of flame is in impingement heating. The direct contact with the flame and the heating object enhances convective heat transfer [7–9]. As far as impinging flame is concerned, there are many investigations on impinging premixed flames, from a round jet or a row of round jets [10–16] and even from slot jet [17,18] the flammability range of premixed burner is small and the effective heating area is relatively small. Premixed burners are rarely used in industrial purpose for safety reasons. On the other hand, impinging diffusion flame burner with high Reynolds Number

* Corresponding author. Tel.: +852-2766-6651; fax: +852-2365-4703.
E-mail address: mmcwl@polyu.edu.hk (C.W. Leung).

0017-9310/$ - see front matter © 2004 Elsevier Ltd. All rights reserved.
doi:10.1016/j.ijheatmasstransfer.2004.02.015

Nomenclature

H	distance between the nozzle and the impingement plate (mm)
IDF	inverse diffusion flame
LPG	liquefied petroleum gas
Re	Reynolds number $=\frac{ud}{v}$
d	diameter of the air port (mm)
r	radial distance from the centre of the air port (mm)
u	velocity of air jet (m/s)
v	kinematic viscosity
z	vertical distance from the surface of the burner port (mm)

Greek symbol

Φ	equivalence ratio $\left(\frac{\text{Stoichiometric air/fuel ratio}}{\text{Actual air/fuel ratio}}\right)$

has long been used in the industrial rapid-heat transfer furnace but the formation of soot is an associated problem. The application of the impinging IDF for impingement heating has not been investigated. However, its application to industrial heating may give a cleaner flame than the diffusion flame and give a wider range of flammability than the premixed flame, and hence worth investigation.

2. Experimenal setup and method

The flame holder and heat flux measurement system were shown in Fig. 1. The flame holder used in the present study was made of copper. There are 12 outer fuel jets, of 2.4 mm diameter each, surrounding a central air jet of 6 mm diameter. The center-to-center distance between the air jet and the fuel jets was 11.5 mm. Butane

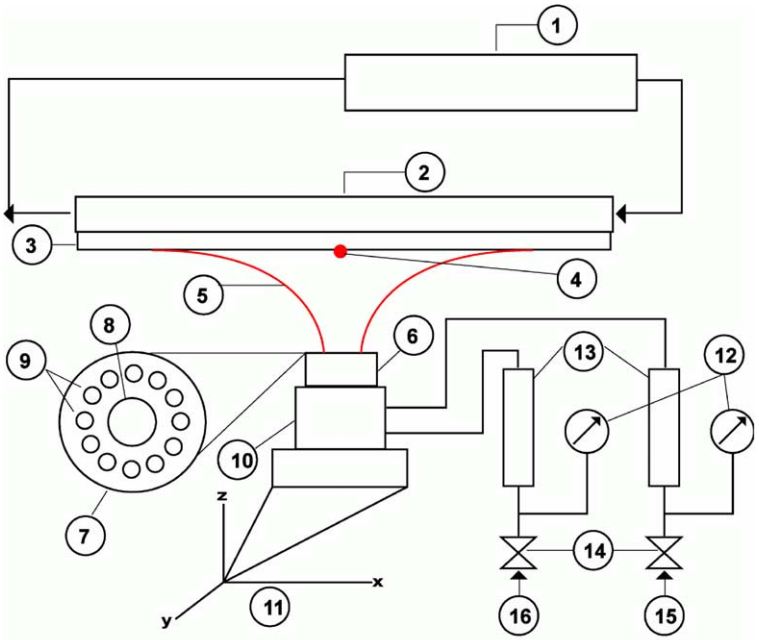

Fig. 1. Schematic of the experimental setup.

and compressed air were metered by rotameters and passed through the corresponding jets. The flame holder was fixed on a positioning system so that the burner could be moved in all directions.

Experiments were carried out in two stages. First, temperature distribution of the flame under Reynolds numbers of 1500, 2000, 2500 and 3000 were measured. The *Re* is that of the air jet. Lower *Re* was not used because the flame became unstable and combustion was incomplete due to poor entrainment force provided by the air jet. Soot formation occurred which could affect the accuracy of the temperature and heat flux measurements. For each *Re*, the air flow rate was fixed and the fuel flow rate adjusted for different Φ ranging from 1.0 to 2.4.

An uncoated type B thermocouple with Pt-30%/Rh as the positive lead and Pt-6%/Rh as the negative lead was used in the experiment. The wire diameter was 0.25 mm. The burner was moved in the *r*-direction with 1 mm interval from $r = 0$ to 30 mm. The burner was also moved in the *z*-direction with 5 mm interval for $z = 0$ to 20 mm and 10 mm interval for $z = 30$–160 mm. The temperatures shown in this paper were corrected according to [16,19] for the radiation effect; the maximum temperature correction was 154 °C in the present study.

Experiments were then carried out on the heat flux measurement system. The system consisted of a water-cooled copper plate with a surface area of 500×500 mm^2 and a thickness of 8 mm. Water adjusted to 38 °C, to avoid water condensing on the copper plate, was used to cool the heat flux sensor and to absorb the heat released by the flame. The IDF impinged on the copper plate and a heat flux transducer was located at the center of the plate to measure the heat flux. The burner was moved in the *r*-direction from $r = 0$ mm to 50 mm. The same heat flux sensor and heat flux measurement method were used in [18]. The sensor is a small ceramic heat flux transducer (Vatell Corporation, Model HFM-6 D/H) with an effective sensing area of 2×2 mm^2 and negligible thickness. It measures the total heat flux due to convection and radiation.

An uncertainty analysis was carried out with the method proposed by [20]. Using a 95% confidence level, the maximum uncertainty in local heat flux was 13%. The maximum and minimum standard deviations of the local heat flux were 14% and 3% respectively.

3. Shape and temperature profile of IDF

The energy content of a flame is highly related to its temperature level and temperature distribution. The shape of a flame will be highly modified upon impingement on a plate. The part of the flame below the plate will be less affected, while the part above will be highly distorted, spreading horizontally along the plate rather than upwards. The heat flux distribution is hence highly dependent on the temperature level of the flame below the plate. Therefore, there is a strong correlation between the two. It is hence useful to investigate the temperature distribution of the open flame and use the results to compare with the heat flux distributions.

Fig. 2a shows the photograph of an inverse diffusion flame at $Re = 2500$ and $\Phi = 1.0$. It shows that the IDF can be consider as making up of an entrainment zone at the root of the flame, of about 10 mm in height, and a subsequent mixing and combustion zone. The whole flame has a visible length of 80 mm. In the entrainment zone, the fuel from the fuel jets is drawn to the central air jet due to the low pressure created by the high velocity air jet. Initial air fuel mixing and combustion occurs in this zone. In the mixing and combustion zone, rapid mixing of air and fuel, and combustion occur. The flame maintains the characteristic yellowish color of a diffusion flame but some regions of bluish flame is also observable at the base, at the top and inside the flame.

Fig. 2b shows the temperature distribution of the flame and the temperature profiles at four heights of 20, 40, 80 and 140 mm at the *z*-direction. The flame was assumed to be symmetrical about the center-line of the air jet, and hence only a half-plane of the flame was measured. There was a neck at the temperature distribution diagram at about $z = 20$ mm, corresponding to the separation between the entrainment zone and the subsequent mixing and combustion zone. High temperature started to occur in the entrainment zone, indicating that combustion occurred in this zone also and propagated upwards. The maximum temperature measured was about 1650 °C, which occurred at the neck region at a distance about midway between the air and fuel ports, indicating that the most intense combustion occurred in this part of the flame.

It can be observed that in the entrainment zone with $z < 20$ mm, the temperature was the lowest at the center of the flame, increasing to a peak at about 5 mm away from the centerline, and then dropped gradually further outwards. At $z = 40$ mm, the temperature was about 1300 °C at the centre, increased further outwards to a maximum of about 1450 °C and then dropped quickly further outwards. At higher levels of $z = 80$ mm and $z = 140$ mm, the temperature was the highest at the center and dropped gradually outwards. The temperature at the centre dropped from 1300 °C at $z = 80$ mm to 650 °C $z = 140$ mm, indicating that the flame was cooling down in between.

The lower centerline temperature at $z < 20$ mm indicates that there was a cool core at the center of the entrainment zone, due to the air jet. The maximum temperature difference in the radial direction within 10 mm was about 1000 °C at $z = 20$ mm, and 120 °C at $z = 40$ mm, indicating a decrease in difference in this

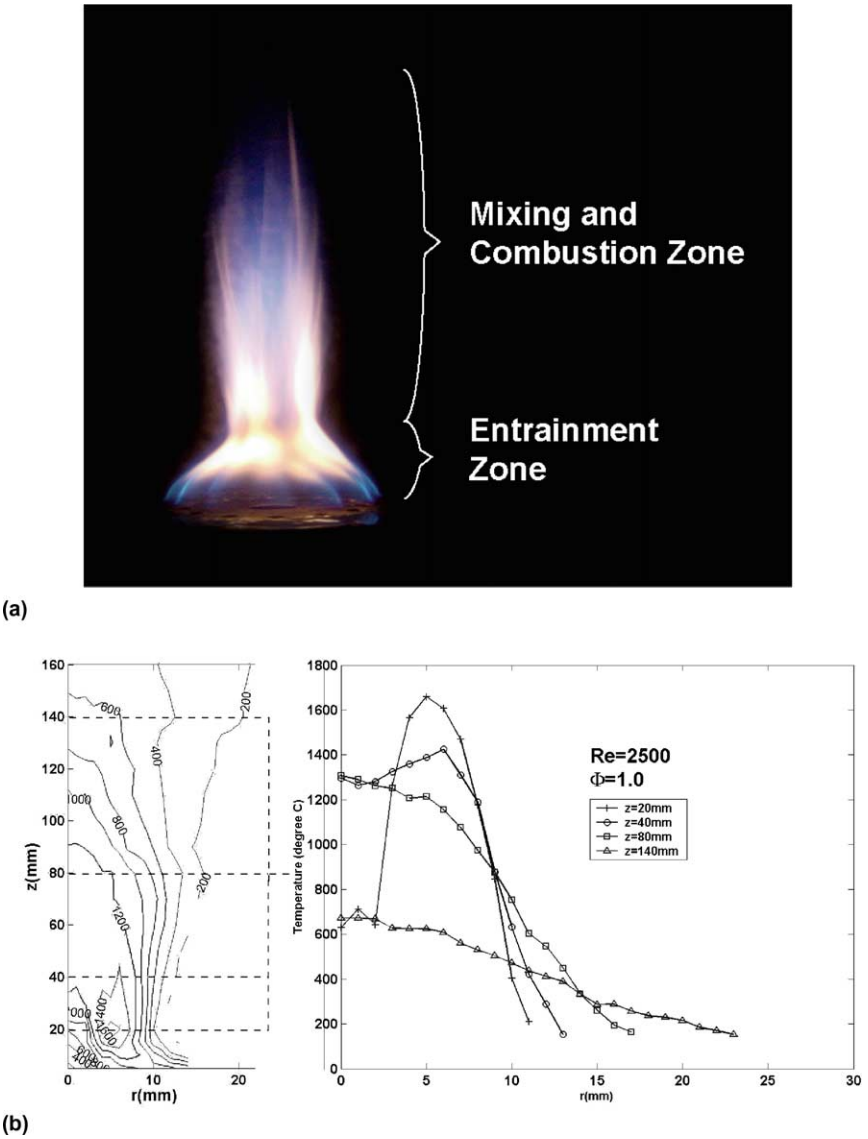

Fig. 2. (a) Structure of an IDF, $Re = 2500$, $\Phi = 1$ and (b) temperature distribution and sectional temperature profiles of an IDF.

region in the upward direction, or a gradual heating up of the air in the core. At the entrainment zone, air jet velocity is very high and the profile is parabolic in shape. Thus the jet velocity is higher at the centerline than that of the edge of the burner. The fuel cannot diffuse into the center of the flame but mixes with the air some way between the air and fuel ports to form a combustible mixture close to stoichiometric composition, and react. Consequently, lean combustion will occur towards the centerline, however, rich combustion will occur towards the fuel ports.

The flame developed in the upward direction and the temperature profiles became bell-shaped at about $z = 80$ mm, which is also the height of the visible flame. The height at which the bell-shaped profile first occurs can be regarded as the end of the combustion zone. The region of the flame beyond can be regarded as the post-combustion and product zone.

Fig. 3 shows the effect of Re and Φ on the flame length. The flame lengths were determined by averaging 10 flame images obtained with a digital camera. The flame lengths were quite stable with individual flame length deviating less than 5% from the mean. An increase in Re at the same Φ value means an increase in both the amount of air supplied and the amount of fuel supplied. An increase in Φ at the same Re means an

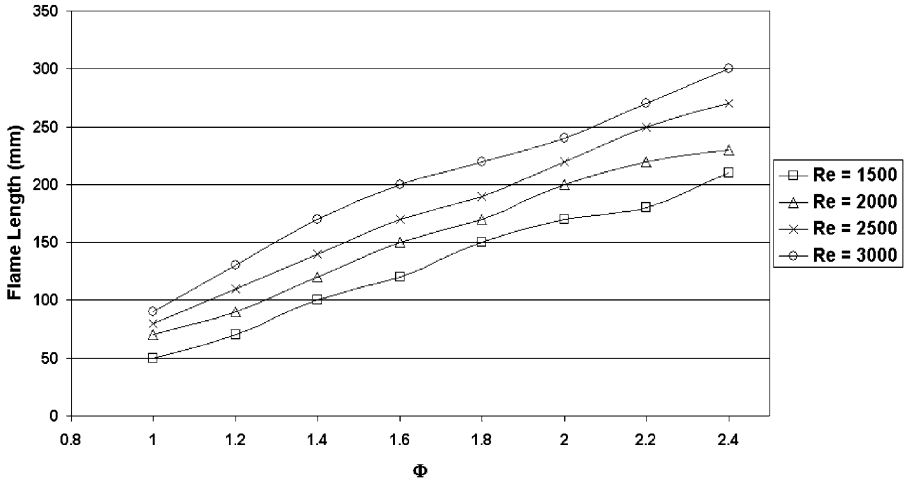

Fig. 3. Flame length vs Φ at different Re.

increase in fuel supplied while the amount of air supplied remains unchanged. The length of the entrainment zone increased slightly with increase in Re and Φ, while the length of the mixing and combustion zone increased significantly with both Re and Φ. In both cases, the increase in length was more dominant with the increase in Φ. The increase in Re at the same equivalence ratio will enhance air fuel mixing which tend to decrease the flame length. However, the increase in fuel supplied will tend to increase the length of the flame, resulting in a net increase in the flame length. The increase in Φ at the same Re will increase fuel supply at the same amount of air, which results in a more significant increase in flame length.

As the combustion was in the fuel-rich region, more fuel was involved in the combustion process and the flame became more diffusion in nature. The time of mixing between air and fuel increased and the length of the mixing and the combustion zone also increased. In very rich flame of $\Phi = 2.0$ and beyond, the flame appeared completely yellowish and unstable. In slightly rich flame, the flame was partially bluish in color and stable.

The IDF is significantly different from the corresponding diffusion and premixed flame. For a diffusion flame of the same fuel flow rate, the flame will be much longer and completely yellowish in color. For a corresponding premixed flame of $Re = 2500$ and $\Phi = 1.0$, the flame will be much shorter and the flame will be bluish in color. Hence, the IDF possesses a different flame structure from the two.

4. Heat flux distribution of impinging IDF

The stagnation point heat flux as well as the distribution of the heat flux along the plate in the radial direction were investigated, under different nozzle-to-plate distances, Re and Φ.

Fig. 4 shows the photographs of the impinging IDF at $Re = 2500$ and $H = 40$ mm. The visible flame length impinged on the plate and spread outwards along the plate. The impingement and spread were not so obvious at $\Phi = 1.0$ but became obvious at $\Phi = 1.4$. The visible length of the open flame at $\Phi = 1.0$ is 80 mm, indicating that the visible part has disappeared upon impinging on and cooled down by the plate. The contact area between the flame and the plate increased with an increase in Φ. The flame became yellowish as the equivalence ratio was increased. When the equivalence ratio was greater than 1.6, the flame became yellowish at the outer zone and bluish in the inner zone. At $\Phi = 2.0$, the flame was nearly totally yellowish in color. The color change of the flame indicates a transition from the nature of premixed combustion to one of diffusion combustion.

4.1. Stagnation point heat flux

4.1.1. Effect of Re and Φ on stagnation point heat flux

The effect of Φ and Re on the stagnation point heat flux is shown in Fig. 5a. Experiments were carried out at $H/d = 7.5$. For each Re, starting at $\Phi = 1.0$, the stagnation point heat flux increased to a peak value and then decreased steadily with further increase in Φ. The shape of the curve is similar to that of a premixed flame in which, theoretically, the peak heat flux should occur at $\Phi = 1.0$ for premixed flame, and drops at both ends. In an impinging IDF, the peak heat flux occurred at much richer condition.

The stagnation point heat flux at $Re = 2000$ was always higher than that at $Re = 1500$. At higher Re of 2500 and 3000, the heat flux was initially higher than those at lower Re as Φ was increased. However, after

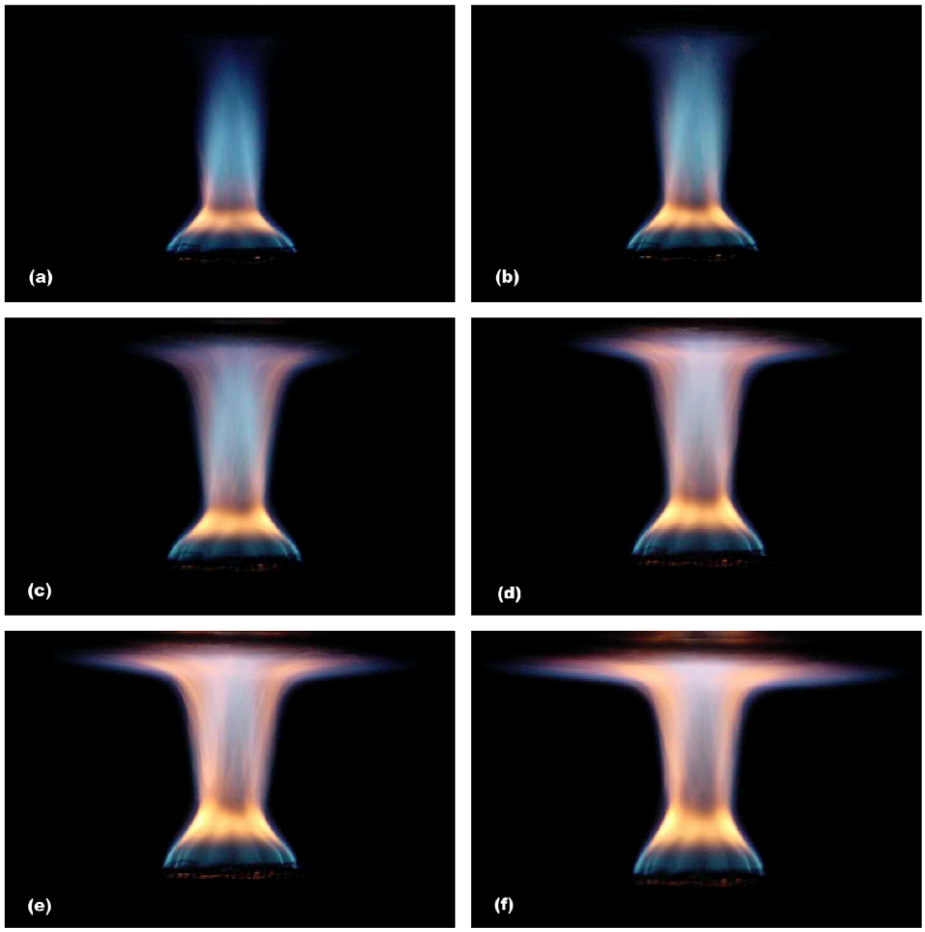

Fig. 4. Shape of impinging IDF, $Re = 2500$: (a) $\Phi = 1.0$; (b) $\Phi = 1.2$; (c) $\Phi = 1.4$; (d) $\Phi = 1.6$; (e) $\Phi = 1.8$ and (f) $\Phi = 2.0$.

reaching the peak value, the heat flux at higher Re dropped heavier than that at lower Re, resulting in lower heat flux at higher Re when Φ was on the high side. Moreover, the peak heat flux occurred at progressively lower Φ at higher Reynolds number.

The results can be explained as follows. The stagnation point heat flux should be related to the temperature at the centerline of the flame. The temperature distribution diagrams of the open IDF show that the centerline temperature of an IDF will increase with z until a peak temperature is reached and then drop gradually. The position of the peak temperature depends on both Re and Φ. With an increase in Re, there will be an increase in flame length and an increase in the high temperature zones, resulting in a higher heat flux at the stagnation point at lower values of Φ, at certain values of H/d. At higher values of Φ, there will be an increase of the flame temperature, and the location of the high temperature zone will shift upwards. However, the impingement flame is now bounded by a plate, at $H/d = 4.5$, which prohibits normal flame development above that height. This height is not sufficient for the good air/fuel mixing and thus flame development, resulting in the drop in heat flux at higher Φ, and the occurrence of the peak heat flux at lower Φ at higher Re.

4.1.2. Effect of nozzle-to-plate distance, H, on stagnation point heat flux

The stagnation point heat flux was measured while the burner was moved at 5 mm interval in z-direction. The minimum distance considered was $H = 10$ mm and the maximum was $H = 100$ mm. The results are shown in Fig. 6b for $Re = 2500$. In the figure, H/d is the nozzle-to-plate distance normalized by the air jet nozzle diameter. The serial lines in the figures represent variation in heat flux at different Φ ranging from 1.0 to 2.4.

In Fig. 5b, the heat flux was very low when H/d was below about 4. At higher H/d, there was an increase in heat flux with H/d. For $\Phi = 1.0$–1.2, the heat flux increased and then leveled off at about $H/d = 10$. For

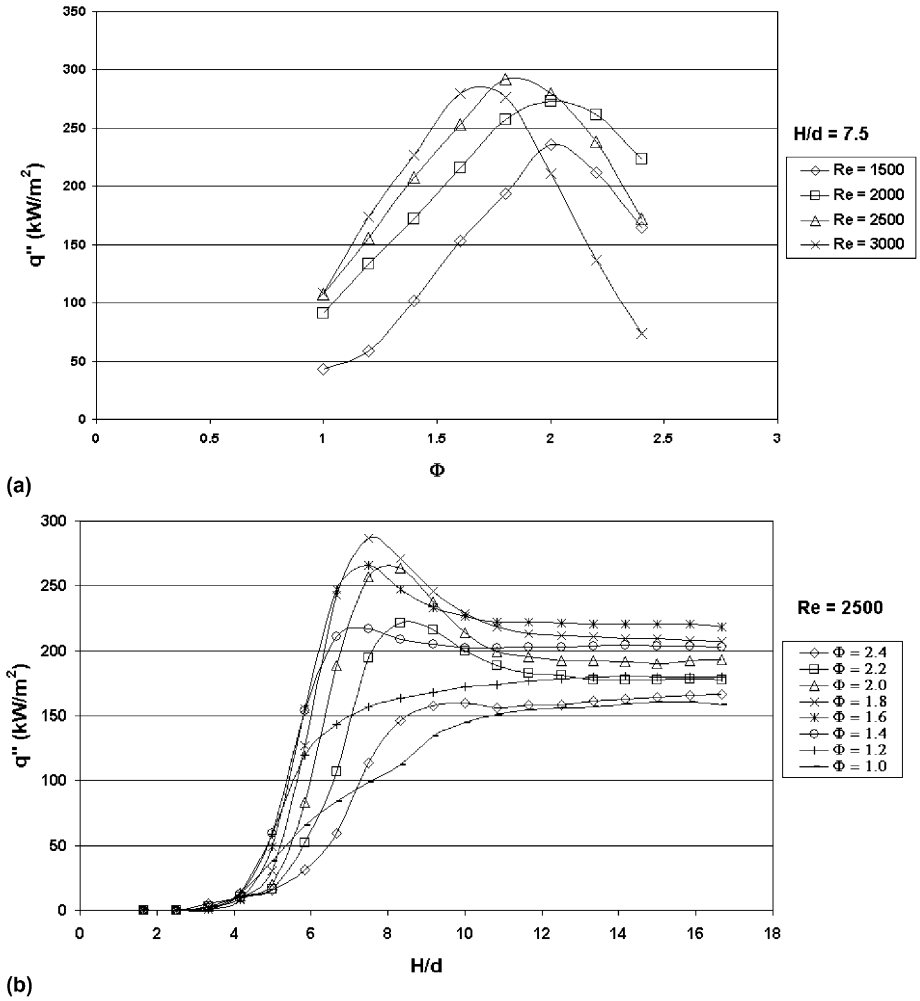

Fig. 5. (a) Variation of stagnation point heat flux with equivalence ratio and *Re* and (b) variation of stagnation point heat flux with H/d and Φ.

$\Phi = 1.4$–2.2, the heat flux increased to a peak value and then dropped off and became steady again at about $H/d = 10$. At $\Phi = 2.4$, the heat flux dropped significantly and did not have an obvious peak. The highest peak heat flux occurred at $\Phi = 1.8$, at $H/d = 7$.

The results can be explained as follows. At H/d of 4 and below, the stagnation point was impinged basically by the air jet, resulting in very low heat flux. At progressively higher values of H/d, there was a corresponding increase in the temperature at the centerline of the flame, as shown in the temperature distribution diagrams of the open IDF, results in an increase of the heat flux. At $\Phi = 1.0$–1.2, the peak temperature of the flame did not occur at the centerline and hence the heat flux increased gradually with H/d. At $\Phi = 1.4$–2.2, the peak temperature of the flame occurred at the centerline and hence the heat flux increased significantly. The increase in Φ was associated with an increase in the length required for mixing and combustion. Upon complete combustion, the centerline temperature dropped again. This resulted in the increase of the heat flux to a peak value and then decrease again. The steady heat flux occurring at $H/d = 10$–17 was unexpected and requires further investigation.

4.2. Radial heat flux distributions

4.2.1. Effect of nozzle-to-plate distance

The radial heat flux distribution at different nozzle-to-plate distance, H, is shown in Fig. 6a, for $\Phi = 1.8$ and $Re = 2500$. In this case, the burner port was fixed at a selected nozzle-to-plate distance and moved with the positioning system along the y-direction. The data points were collected at initially 2 mm interval up to the location $r/d = 5$, and then at 4 mm interval further downstream,

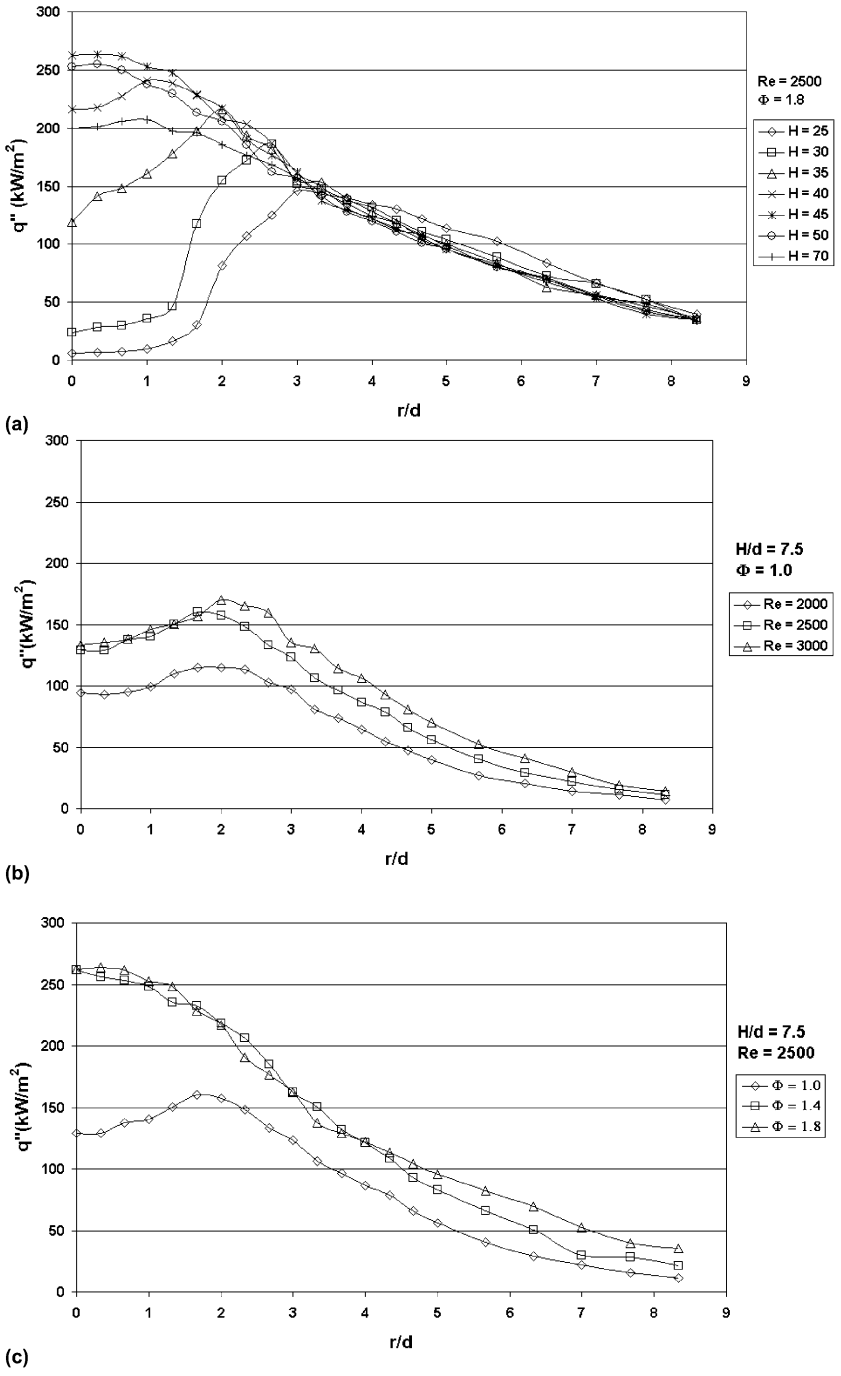

Fig. 6. (a) Effect of H/d on radial heat flux distribution; (b) effect of Re on radial heat flux distribution and (c) effect of Φ on radial heat flux distribution.

until $r = 50$ mm. Fig. 6a shows that the curves can be divided into two groups. For $H = 25$, 30, 35 and 40 mm, the heat flux increased with r/d until a peak value was reached and then dropped steadily as r/d was further increased. The heat flux was higher at higher value of H. The peak heat flux was also higher at higher value of H. The peak heat flux occurred at smaller r/d as H was increased. In another word, the peak heat flux shifted towards the stagnation point as H was increased. The smaller heat flux at the stagnation point indicates the

existence of a cooler core when the flame impinges at the plate with a small nozzle-to-plate distance.

For $H = 45$ mm or more, the peak heat flux occurred at the stagnation point. The cooler core disappeared in these flames. In these cases, the heat flux decreased with increasing distance from the stagnation point. The maximum heat flux at the stagnation point occurred at $H = 45$ mm. At $H = 70$ mm, the heat fluxes at all locations were lower than those at $H = 45$ mm. Hence, it can be concluded that at about $H = 45$, the flame had reached complete completion at the impingement point. At lower H, the flame has not reached complete combustion at the impingement point. At higher H, complete combustion has occurred before reaching the plate, the flame temperature cooled down. In all cases, the heat fluxes were almost the same in $r/d > 3$, indicating that the change in H/d has little effect on the heat flux in this region.

The same was observed with the temperature distribution in an open IDF. At low z, there was a cool core zone. Within the cool core zone, the temperature was low at the centerline but increased to a peak value at some distance away. The location of this peak temperature also shifted towards the centerline at higher flame heights.

4.2.2. Effect of Φ and Re

The effect of *Re* on the radial heat flux distribution is shown in Fig. 6b for $H = 45$ mm, with $\Phi = 1.0$. There was in general an increase in heat flux with an increase of *Re*. The location of the peak heat flux remained at almost the same location of $r/d = 2$. Fig. 6c shows the effect of Φ on the radial heat flux distribution at $H = 45$ mm, with $Re = 2500$. In this case, the cool core effect was observable but to a much less extent at $\Phi = 1.0$. For $\Phi = 1.4$–1.8, the peak heat flux occurred at the stagnation point. The heat flux was almost constant within the region $r/d = 0$ to $r/d = 2$, and then dropped steadily.

It can be concluded that the heat flux distribution is affected by the nozzle-to-plate distance, *Re* and Φ. *Re* will in general increase the heat flux, while there is an optimal nozzle-to-plate distance and an optimal Φ for improved heat flux distribution.

4.2.3. Comparison of heat flux with premixed impingement flame

The characteristics of the heat flux obtained from the IDF were compared with those obtained from premixed impinging flames of Dong et al. [10] and Kwok et al. [18]. The radial heat fluxes obtained in the two types of flame have the same profile and characteristic. However there are certain differences. First premixed flames have higher peak heat flux than IDF especially at stoichiometric and lean conditions. Second in premixed flames, higher peak heat flux is obtained at close to stoichiometric condition while in IDF higher peak heat flux is obtained in rich condition. Third the IDF is more stable than the premixed flame such that they can operate at higher Reynolds number and hence afford higher fuelling rates. Finally the radial decay of the stagnation point heat flux is faster in premixed flames than in IDF; hence the IDF has more uniform heating effect.

4.3. Radial distribution of combustion products

The combustion products, including CO_2, CO, NO and O_2, were measured in this experiment for comparison with the radial heat flux distribution. Combustion products were sampled from a 1 mm hole on the impingement plate. The hole was 50 mm away from the heat flux sensor. A 5-gas analyzer (Anapol EU-200/4) was used for measuring the species concentrations. The analyzer uses IR sensor for measuring the CO_2 concentrations and electro-chemical sensors for CO, NO and O_2 concentrations. The CO_2, CO and O_2 concentration were measured in percentage (%) and the NO concentration in ppm. The data were collected at 1 mm interval in the radial direction, up to $r = 50$ mm.

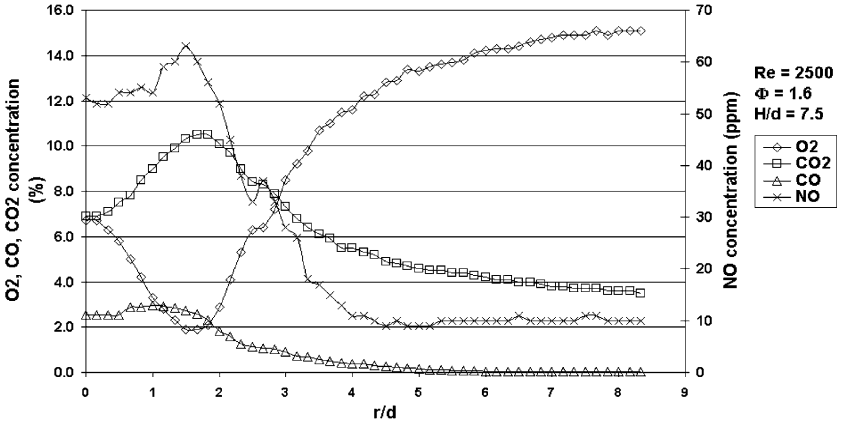

Fig. 7. Species concentrations in radial direction.

Fig. 7 shows the results, for the case $Re = 2500$, $\Phi = 1.6$ and $H/d = 7.5$. The CO_2 concentration was 7% at $r/d = 0$, rising steadily to the peak value of 10.5% at $r/d = 1.8$ and then dropped again. The trend of the CO concentration was the same as that of the CO_2 concentration. The CO concentration was 2.5% at the stagnation point, rising to a peak value of 3% at $r/d = 1.8$ and then dropped to zero further outwards. NO also increased to a peak value at $r/d = 1.8$ and then dropped sharply afterwards until it reached a steady value of 10 ppm. On the other hand, the O_2 concentration decreased to a minimum value at $r/d = 1.8$ and the increased steadily to about 15% at $r/d = 8$.

The CO_2, CO and NO concentrations reached their peak values at $r/d = 1.8$ while the O_2 concentration reached its minimum value at the same location. The results indicate that at $H/d = 7.5$, combustion was the most intense at the location $r/d = 1.8$. It shows agreement with the result in the radial heat flux distribution in which the peak heat flux occurred within the region of $r/d = 2$. Within this region, combustion was in progress and should have been completed. Beyond that, the plate was heated up by the combustion products.

5. Conclusion

In the present study, the temperature distribution and the heat flux distribution of an inverse diffusion flame was investigated. The following results are obtained.

1. Basically, the IDF consists of entrainment zone and the mixing and combustion zone. At low Φ, a blue flame with short mixing and combustion zone is observed. At high Φ, a yellowish flame with long mixing and combustion zone is observed. An increase in Re also increases the length of the mixing and combustion zone. The length of the entrainment zone is not much affect by either Re or Φ.
2. The temperature profiles at different sections of the flame show a cool core at low flame heights. At high flame height the cool core disappear and the maximum temperature zone occurred at the centre and dropped steadily away from the centre.
3. The stagnation point heat flux is greatly affected by three factors: Re, Φ, and the nozzle to plate distance. In order to generate the highest stagnation point heat flux, both Φ and Re have to be adjusted at a fixed nozzle-to-plate distance. At higher Re, the peak heat flux occurs at lower Φ, and at a lower value of H/d.
4. The radial heat flux distribution is affected by the nozzle-to-plate distance, Re and Φ. Re will in general increase the heat flux, while there is an optimal nozzle-to-plate distance and an optimal Φ for improved heat flux distribution.At very low values of H, the peak heat flux occurs at a distance away from the stagnation point due to the cool core of the flame. At high values of H, the peak heat flux occurs at the stagnation point.
5. In comparison with premixed impingement flame, the IDF has lower peak heat flux but can provide higher fuelling rate and more uniform heating around the stagnation point.
6. The radial distribution of the combustion products shows that intense reaction occurs in a region which corresponds to the region of high heat flux. The heat flux drops in the post-combustion regions.

Acknowledgements

The authors wish to thank the Hong Kong Polytechnic University for financial support of the present study.

References

[1] A. Cavaliere, R. Ragucci, Gaeous diffusion flames: simple structures and their interaction, Progr. Energy Combust. Sci. (27) (2001) 547–585.
[2] K.T. Wu, The Comparative structure of normal and inverse diffusion flames, Ph.D. Thesis, The Ohio State University, 1984.
[3] Y. Bindar, A. Irawan, Size and structure of LPG and hydrogen inverse diffusion flames at high level of fuel excess, in: Proceedings of the 6th Asis-Pacific International Symposium on Combustion and Energy Utilization, 2002, pp. 124–130.
[4] E.M. Clausing, S.W. Senser, N.M. Laurendeau, Peclet correlation for stability of inverse diffusion flames in methane-air cross flows, Combust. Flame 110 (1997) 405–408.
[5] T. Takagi, Z. Xu, M. Komiyama, Preferential diffusion effects on the temperature in usual and inverse diffusion flames, Combust. Flame 106 (1996) 252–260.
[6] G.W. Sidebotham, I. Glassman, Flame temperature, fuel Structure, and fuel concentration effects on soot formation in inverse diffusion flames, Combust. Flame 90 (1992) 269–283.
[7] J.W. Mohr, J. Seyed-yagoobi, R.H. Page, Combustion measurements from an impinging radial jet reattachment flame, Combust. Flame 106 (1996) 69–80.
[8] J. Wu, J. Seyed-yagoobi, R.H. Page, Heat transfer and combustion characteristics of an array of radial jet reattachment flames, Combust. Flame 125 (2001) 955–964.
[9] E.H. Comfort, T.J.O. Connor, L.A. Cass, Heat transfer resulting form the normal impingement of a turbulent high temperature jet on an infinitely large plate, in: Proceedings of the 1966 Heat Transfer and Fluid Mechanics Institute, 1996, pp. 44–62.
[10] L.L. Dong, C.S. Cheung, C.W. Leung, Heat transfer characteristics of an impinging butane/air flame jet of low

Reynolds number, Exper. Heat Transfer 14 (2001) 265–282.
[11] L.L. Dong, C.W. Leung, C.S. Cheung, Heat transfer characteristics of premixed butane/air flame jet impinging on an inclined flat surface, Heat Mass Transfer 39 (2002) 19–26.
[12] L.L. Dong, C.W. Leung, C.S. Cheung, Heat transfer of a row of three butane/air flame jets impinging on a flat plate, Int. J. Heat Mass Transfer 46 (2003) 113–125.
[13] G.K. Hargrave, M. Fairweather, J.K. Kilham, Forced convective heat transfer from premixed flames—Part 2: impinging heat transfer, Heat Fluid Flow 8 (1987) 132–138.
[14] Th.H. Van der Meer, Stagnation point heat transfer from turbulent low Reynolds number jets and flame jets, Exper. Therm. Fluid Sci. 4 (1991) 115–126.
[15] Y. Zhang, K.N.C. Bray, Characterization of impinging jet flames, Combust. Flame 116 (1999) 671–674.
[16] C.E. Baukal, Heat Transfer in Industrial Combustion, CRC Press, Boca Raton, FL, 2000.
[17] L.L. Dong, C.S. Cheung, C.W. Leung, Heat transfer from an impinging premixed butane/air slot flame jet, Int. J. Heat Mass Transfer 45 (2002) 979–992.
[18] L.C. Kwok, C.W. Leung, C.S. Cheung, Heat transfer characteristics of slot and round premixed impinging flame jets, Exper. Heat Transfer 16 (2003) 111–137.
[19] A. Sato, A correctional calculation method for thermocouple measurements of temperature in flames, Combust. Flame 24 (1975) 35–41.
[20] S.J. Kline, F.A. McClintock, Describing uncertainties in single-sample experiments, Mech. Eng. 75 (1953) 3–8.